FABAD J. Pharm. Sci., 47, 3, 347-360, 2022
Doi: 10.55262/fabadeczacilik.1128446
RESEARCH ARTICLE

Novel (p-Tolyl)-3(2H)-Pyridazinone Derivatives Containing Substituted-1,2,3-Triazole Moiety as New Anti-Alzheimer Agents: Synthesis, *In vitro* and *In silico* Assays

İrem BOZBEY MERDE[*°], Gülce TAŞKOR ÖNEL[**], Burçin TÜRKMENOĞLU[***], Şule GÜRSOY[****], Esra DİLEK[*****]

Novel (p-Tolyl)-3(2H)-Pyridazinone Derivatives Containing Substituted-1,2,3-Triazole Moiety as New Anti-Alzheimer Agents: Synthesis, In vitro and In silico Assays

SUMMARY

Alzheimer's disease (AD) is a chronic neurodegenerative disease that is the most common cause of dementia. The risk of developing the disease increases with age. When the histopathology of the disease is examined, senile amyloid plaques, neurofibrillary tangle formation, synapse-neuron loss, and marked atrophy in the brain are detected. The decrease in the level of choline acetyltransferase, which is responsible for the synthesis of acetylcholine in Alzheimer's disease, is 58-90%. There is a great need for new drugs that target the basis of the cause of the disease, as existing drugs cannot stop the progression of the disease. In this study, triazole-pyridazinone derivative compounds showing acetylcholinesterase inhibition were synthesized and their inhibitions were investigated. Compound 6e exhibited the strongest inhibitory effect with a Ki value of 0.049 ± 0.014 μM (Tacrine Ki= 0.226 ± 0.025 μM). In addition, in silico studies were applied for all compounds.

Keywords: *3(2H)-pyridazinone, acetylcholinesterase, molecular docking*

1,2,3-Triazol Uygulaması Yeni Anti-Alzheimer (P-Tolil)-3(2H)-Piridazinon Türevleri: Sentez Çalışmaları, in vitro ve in siliko Analizleri

ÖZ

Alzheimer hastalığı (AH), demansın en yaygın nedeni olan kronik nörodejeneratif bir hastalıktır. Hastalığa yakalanma riski yaşla birlikte artar. Hastalığın histopatolojisi incelendiğinde senil amiloid plakları, nörofibriler yumak oluşumu, sinaps-nöron kaybı ve beyinde belirgin atrofi saptanır. Alzheimer hastalığında asetilkolin sentezinden sorumlu olan kolin asetil transferaz düzeyindeki azalma %58-90'dır. Mevcut ilaçlar hastalığın ilerlemesini durduramadığından, hastalığın temel nedenini hedef alan yeni ilaçlara büyük ihtiyaç vardır. Bu çalışmada asetilkolinesteraz inhibisyonu gösteren triazol-piridazinon türevi bileşikler sentezlenmiştir ve enzim inhibisyonları araştırılmıştır. Bileşik 6e, 0.049 ± 0.014 μM Ki değeri ile en güçlü inhibitör etkiyi göstermiştir (Takrin Ki= 0.226 ± 0.025 μM). Ayrıca sentezlenen tüm bileşikler için in siliko çalışmalar yapıldı.

Anahtar Kelimeler: *3(2H)-piridazinon, asetilkolinesteraz, moleküler yerleştirme*

Received: 9.06.2022
Revised: 03.08.2022
Accepted: 4.08.2022

* ORCID: 0000-0002-9290-938X, Erzincan Binali Yıldırım University, Department of Pharmaceutical Chemistry, Erzincan, Turkey
** ORCID: 0000-0002-9375-2329, Erzincan Binali Yıldırım University, Department of Analytical Chemistry, Erzincan, Turkey
***ORCID: 0000-0002-5770-0847, Erzincan Binali Yıldırım University, Department of Analytical Chemistry, Erzincan, Turkey
**** ORCID: 0000-0001-5236-5974, Erzincan Binali Yıldırım University, Department of Biochemistry, Erzincan, Turkey
*****ORCID: 0000-0002-3629-5168, Erzincan Binali Yıldırım University, Department of Biochemistry, Erzincan, Turkey

° Corresponding Author; İrem BOZBEY MERDE
Phone: +90 446 224 53 44, Fax: +90 446 224 53 43, e.mail: irem.bozbey@erzincan.edu.tr, irembzby@gmail.com

INTRODUCTION

Alzheimer's disease (AD) is an age-related progressive neurodegenerative disease that is characterized by cognitive impairment, has a high incidence in the elderly, and gradually results in death (Arora, Alfulaij, Higa, Panee, & Nichols, 2013; Daulatzai, 2016; Kumar, Kumar, Keegan, & Deshmukh, 2018). Today, around 50 million people worldwide, especially older people, suffer from dementia. According to estimates, the number of patients between 2040 and 2050 is reported to be approximately 130 million. Most dementia cases (70%) are due to AD (Cummings, Lee, Zhong, Fonseca, & Taghva, 2021; Taudorf, Nørgaard, Waldemar, & Laursen, 2021). Histopathologically, AD is characterized by loss of cholinergic neurons, amyloid b (Ab) peptide deposits (plaques), and intracellular neurofibrillary tangles of tau protein. Therefore, they have become important drug development targets (Cummings et al., 2021; Huang, Chao, & Hu, 2020; Taudorf et al., 2021). Currently, there is no treatment available to cure AD and stop its progression. The drugs are used to reduce the problems that occur in patients' ability to understand and comprehend behavioral findings (Srivastava, Ahmad, & Khare, 2021). When the brain tissues of AD patients were examined, it was shown that there was a decrease in acetylcholine synthesis and release and a decrease in acetylcholine transferase activity (Fani Maleki et al., 2020; Koronyo-Hamaoui et al., 2020; Zhang et al., 2020). For this purpose, acetylcholinesterase inhibitors have been developed to increase the residence time of acetylcholine in the synaptic gap (Birks, 2006).

In our previous studies, we synthesized a series of 3(2*H*)-pyridazinone derivatives and it has been reported that have been anticholinesterase biological activities (Bozbey et al., 2020; Çöl, Bozbey, Türkmenoğlu, & Uysal, 2022b; Özçelik, Özdemir, Sari, Utku, & Uysal, 2019). Likewise, the anticholinesterase effects of triazole structures have also been widely reported in the literature (Hosseini, Pourmousavi, Mahdavi, & Taslimi, 2022; Krasiński et al., 2005; Mina Saeedi et al., 2021; M. Saeedi et al., 2017). In the light of all this information, the combination of two bioactive compounds, triazole and pyridazinone, can be considered a significant strategy for drug design and discovery. Within the scope of our study, five novel triazole ring-substituted derivatives were synthesized, evaluated their acetylcholinesterase (AChE) enzyme inhibition, and *in silico* studies were performed.

MATERIALS AND METHODS

Chemistry

Unless otherwise noted, all of the reagents were commercial quality and were used without purification. The progress of reactions and the purity of the compounds were monitored by TLC using silica gel plates (250 μm, F_{254}) under UV light. NMR spectra were recorded on an Agilent Varian Mercury 400 MHz (^{1}H, 400 MHz; ^{13}C, 100 MHz), in $CDCl_3$ and DMSO-d_6 (internal standard tetramethylsilane). Chemical shifts (δ) are expressed as parts per million (ppm) downfield from tetramethylsilane (TMS) and the coupling constants (*J*) quoted in Hertz. Splitting patterns have been designated as follows: s (singlet), d (doublet), t (triplet) and m (multiplet), br (broad). The IR Spectra were recorded on Thermo Scientific Nicolet 6700 ATR/Fourier transform infrared spectrophotometer. High-resolution mass spectra data (HRMS) were collected in sing a Waters LCT Premier XE Mass Spectrometer (high sensitivity orthogonal acceleration time flight instrument) operating in the ESI (+) method, also coupled to an AQUITY Ultra Performance Liquid Chromatography system (Waters Corporation, Milford, MA, USA).

General procedure for the preparation of compounds (1) and (2)

The substituted 4'-methylacetophenone (1 mmol), glyoxylic acid monohydrate (1 mmol), and acetic acid (2 mL) were heated and stirred under reflux for 5 h. After the reaction was completed, the reaction mix-

ture cooled down to room temperature, and 20 mL of water and ammonium hydroxide solution (25%) were added until the medium pH became 8. Then the reaction mixture was extracted with dichloromethane (3x20 mL). To the aqueous layer was added hydrazine hydrate (10 mmol) and the reaction mixture was refluxed for 3 h. After completion of the reaction, the reaction mixture cooled down to room temperature. The resulting white precipitate was filtered and recrystallized from ethanol (Xu et al., 2016).

General procedure for the preparation of compound (3)

A solution of **(2)** (1 mmol), K_2CO_3 (3 mmol), and ethyl 3-bromopropionate (3 mmol) in acetone (20 mL) was heated and stirred under reflux for 12 h. After the reaction was completed, the reaction mixture cooled down to room temperature. The resulting mixture was poured into ice-water, filtered off, and washed thoroughly with water. The resulting precipitate **(3)** was recrystallized from ethanol (Mantu, Luca, Moldoveanu, Zbancioc, & Mangalagiu, 2010).

General procedure for the preparation of compound (4)

To a solution of **(3)**, (1 mmol) in ethanol (20 ml) was added hydrazine hydrate (5 mmol). The reaction mixture was heated under reflux for 1 h. The precipitate obtained was washed thoroughly with water, dried, and recrystallized from methanol (Hassanien, 2003).

General procedure for the preparation of compounds 5, 6 (a-e)

A reaction mixture of appropriate hydrazide **(4)** (1 mmol) and aryl isothiocyanate (1 mmol) in ethanol (25 mL) was heated under reflux for 5 h and the progress of the reaction was monitored by thin layer chromatography. Next, the solution was cooled and the solid formed was filtered off, washed with diethyl ether, dried, and crystallized from ethanol. After, synthesized derivatives of thiocarbazide (1 mmol) were dissolved in the 2% solution of sodium hydroxide (20 mL) and heated under reflux for 4 h. After cooling, the solution was neutralized with dilute HCl. The precipitate was filtered off and then recrystallized from ethanol (Hassanien, 2003; Onkol et al., 2008).

2-(2-(4-phenyl-5-thioxo-4,5-dihydro-1*H*-1,2,4-triazol-3-yl)ethyl)-6-(*p*-tolyl)pyridazin-3(2*H*)-one (6a)

White solid (52% yield), R_f 0.53 (CH_3OH-$CHCl_3$ 9:1), mp 125-127˚C, ^{1}H NMR (400 MHz, $CDCl_3$) δ_H 11.72 (s, 1H, -NH), 7.58 (d, 1H, J=8.0 Hz, 5-CH), 7.51 (d, 2H, J=8.0 Hz, 2›- & 6›-CH), 7.48-7.39 (m, 3H, Ph-H), 7.34 (d, 2H, J=8.0 Hz, Ph-H), 7.24 (d, 2H, J=8.0 Hz, 3'- & 5'-CH), 6.92 (d, 1H, J=8.0 Hz, 4-H), 3.75 (t, 2H, J=4.0 Hz, -CH_2-), 2.98 (t, 2H, J=4.0 Hz, -CH_2-), 2.39 (s, 3H, -CH_3), ^{13}C NMR (100 MHz, $CDCl_3$) δ_C 160.82 (5"-C), 145.93 (3-C), 141.01 (3"-C), 133.37 (6-C), 130.99 (4'-C), 130.36, 130.11, 129.76, 127.27 (Ph-C), 129.86 (2'-, 3'-, 5'- & 6'-C), 125.90 (4- & 5-C), 47.12 (-CH_2-), 26.55 (-CH_2-), 21.85 (-CH_3), FT-IR (neat, cm^{-1}) 3220.20, 2948.89, 1635.87 (C=O), 1573.71, 1416.03, 1125.45 (C=S), MS m/z (ESI) calcd for $C_{21}H_{19}N_5OS$ ($M+H^+$) 390.1389, found 390.1395.

2-(2-(4-(4-bromophenyl)-5-thioxo-4,5-dihydro-1*H*-1,2,4-triazol-3-yl)ethyl)-6-(*p*-tolyl)pyridazin-3(2*H*)-one (6b)

White solid (42% yield), R_f 0.55 (CH_3OH-$CHCl_3$ 9:1), ^{1}H NMR (400 MHz, DMSO-d_6) δ_H 13.02 (s, 1H, -N*H*), 7.95 (d, 1H, *J*=8.0 Hz, 5-C*H*), 7.65 (d, 4H, *J*=8.0 Hz, 2'-, 6'-C*H* & Ph-*H*), 7.28 (d, 4H, *J*=8.0 Hz, 3'-, 5'-C*H*, Ph-*H*), 6.94 (d, 1H, *J*=8.0 Hz, 4-*H*), 4.19 (t, 2H, *J*=4.0 Hz, -CH_2-), 2.91 (t, 2H, *J*=4.0 Hz, -CH_2-), 2.34 (s, 3H, -CH_3), ^{13}C NMR (100 MHz, DMSO-d_6) δ_C 167.53 (5"-*C*), 159.11 (3-*C*), 148.08 (3"-*C*), 144.03 (6-*C*), 139.42 (4'-*C*), 135.99, 132.18, 130.88, 129.97 (Ph-*C*), 126.17 (2'-, 3'-, 5'- & 6'-*C*), 121.42 (4- & 5-*C*), 48.99 (-*C*H_2-), 25.32 (-*C*H_2-), 21.32 (-*C*H_3), FT-IR (neat, cm^{-1}) 3184.37, 3021.94, 1648.16 (C=O), 1579.49, 1439.92, 1164.97 (C=S), MS *m/z* (ESI) calcd for $C_{21}H_{19}N_5OSBr$ ($M+H^+$) 468.0494, found 468.0494.

2-(2-(5-thioxo-4-(*p*-tolyl)-4,5-dihydro-1*H*-1,2,4-triazol-3-yl)ethyl)-6-(*p*-tolyl)pyridazin-3(2*H*)-one (6c)

White solid (61% yield), R_f 0.59 (CH_3OH-$CHCl_3$ 9:1), ^{1}H NMR (400 MHz, DMSO-d_6) δ_H 13.60 (s, 1H, -N*H*), 7.93 (d, 1H, *J*=8.0 Hz, 5-C*H*), 7.63 (d, 2H, *J*=8.0 Hz, 2'- & 6'-C*H*), 7.31 (d, 2H, *J*=8.0 Hz, 3'-, 5'-C*H*), 7.26 (d, 4H, *J*=8.0 Hz, Ph-*H*), 6.94 (d, 1H, *J*=8.0 Hz, 4-*H*), 4.20 (t, 2H, *J*=4.0 Hz, -CH_2-), 2.96 (t, 2H, *J*=4.0 Hz, -CH_2-), 2.47 (s, 3H, -CH_3), 2.34 (s, 3H, -CH_3), ^{13}C NMR (100 MHz, DMSO-d_6) δ_C 168.41 (5"-*C*), 159.33 (3-*C*), 150.26 (3"-*C*), 144.38 (6-*C*), 139.92 (4'-*C*), 139.72, 132.00, 131.67, 130.81, 130.47, 130.01 (Ph-*C*), 128.78, 128.41 (2'-, 3'-, 5'- & 6'-*C*), 126.35 (4- & 5-*C*), 48.38 (-*C*H_2-), 25.22 (-*C*H_2-), 21.50 (-*C*H_3), 21.45 (-*C*H_3), FT-IR (neat, cm^{-1}) 3145.81, 3043.49, 2918.67, 2851.42, 1654.35 (C=O), 1586.50, 1412.93, 1127.07 (C=S), MS *m/z* (ESI) calcd for $C_{22}H_{21}N_5OS$ ($M+H^+$) 404.1545, found 404.1541.

2-(2-(4-(2-methoxyphenyl)-5-thioxo-4,5-dihydro-1*H*-1,2,4-triazol-3-yl)ethyl)-6-(*p*-tolyl)pyridazin-3(2*H*)-one (6d)

White solid (38% yield), R_f 0.53 (CH_3OH-$CHCl_3$ 9:1), ^{1}H NMR (400 MHz, DMSO-d_6) δ_H 13.67 (s, 1H, -N*H*), 7.97 (d, 1H, *J*=8.0 Hz, 5-C*H*), 7.66 (d, 2H, *J*=8.0 Hz, 2›- & 6›-C*H*), 7.52 (t, 1H, *J*=8.0 Hz, Ph-*H*), 7.32-7.25 (m, 4H, 3'-, 5'-C*H* & Ph-*H*), 7.10 (t, 1H, *J*=4.0 Hz, Ph-*H*), 7.24 (d, 2H, *J*=8.0 Hz, 3'- & 5'-C*H*), 6.97 (d, 1H, *J*=8.0 Hz, 4-*H*), 3.76 (s, 3H, -OCH_3), 2.89 (m, 2H, -CH_2-), 2.78 (m, 2H, -CH_2-), 2.34 (s, 3H, -CH_3), ^{13}C NMR (100 MHz, DMSO-d_6) δ_C 168.49 (5"-*C*), 159.15 (3-*C*), 154.97 (Ph-*C*-OCH$_3$), 150.33 (3"-*C*), 144.12 (6-*C*), 139.55 (4'-*C*), 131.88, 129.96, 122.18, 121.27 (Ph-*C*), 126.14 (2'-, 3'-, 5'- & 6'-*C*), 113.31 (4- & 5-*C*), 56.37 (-O*C*H$_3$), 48.17 (-*C*H_2-), 24.66 (-*C*H_2-), 21.29 (-*C*H_3), FT-IR (neat, cm^{-1}) 3037.70, 2919.72, 1648.05 (C=O), 1581.69, 1463.50, 1155.46 (C=S), MS *m/z* (ESI) calcd for $C_{22}H_{21}N_5O_2S$ ($M+H^+$) 420.1494, found 420.1496.

2-(2-(5-thioxo-4-(4-(trifluoromethoxy)phenyl)-4,5-dihydro-1*H*-1,2,4-triazol-3-yl)ethyl)-6-(*p*-tolyl)pyridazin-3(2*H*)-one (6e)

White solid (69% yield), R_f 0.49 (CH_3OH-$CHCl_3$ 9:1), ^{1}H NMR (400 MHz, DMSO-d_6) δ_H 13.08 (s, 1H, -N*H*), 7.92 (d, 1H, *J*=8.0 Hz, 5-C*H*), 7.64 (d, 2H, *J*=8.0 Hz, 2'- & 6'-C*H*), 7.41 (d, 4H, *J*=8.0 Hz, Ph-*H*), 7.26 (d, 2H, *J*=8.0 Hz, 3'-, 5'-C*H*), 6.92 (d, 1H, *J*=8.0 Hz, 4-*H*), 4.20 (t, 2H, *J*=4.0 Hz, -CH_2-), 2.89 (t, 2H, *J*=4.0 Hz, -CH_2-), 2.34 (s, 3H, -CH_3), ^{13}C NMR (100 MHz, DMSO-d_6) δ_C 167.33 (5"-*C*), 159.07 (3-*C*), 147.54 (3"-*C*), 143.97 (6-*C*), 139.35 (4'-*C*), 136.64, 132.03, 130.56, 129.90 (Ph-*C*), 130.82 (-O*C*F$_3$), 126.18 (2'-, 3'-, 5'- & 6'-*C*), 121.46 (4- & 5-*C*), 49.32 (-*C*H_2-), 25.42 (-*C*H_2-), 21.29 (-*C*H_3), FT-IR (neat, cm^{-1}) 3038.88, 2926.27, 1654.81 (C=O), 1585.96, 1442.30, 1154.85 (C=S), MS *m/z* (ESI) calcd for $C_{22}H_{18}F_3N_5O_2S$ ($M+H^+$) 474.1212, found 474.1211.

Acetylcholinesterase (AChE) Enzyme Inhibition Studies

AChE enzyme was supplied ready-made. AChE enzyme activity was determined according to the method performed by Ellman's et al. (Ellman, Courtney, Andres, & Featherstone, 1961). The AChE enzyme has two substrates, DTNB [(Ellmans Reagent) 5,5-dithio-bis-(2-nitrobenzoic acid)] and acetyltiyocholiniodate. Thiocholine is formed because of the hydrolysis of the substrates. The thiocholine formed reacts with DTNB and forms the yellow 5-thio-2-nitrobenzoate anion. This molecule gives maximum absorbance at 412 nm wavelength (Shirinzadeh, Dilek, & Alım, 2022). A percent activity versus inhibitor concentration graph was drawn for the designation of the inhibition efficacy of each of the new derivatives on the AChE enzyme. The IC_{50} values were obtained from these graphs. For the calculation of K_i values, three different of these compounds concentrations and five substrate concentrations were used. The study also included an inhibition graph of the most effective

compound which was drawn. The same procedures were performed for Tacrine, the standard inhibitor of the AChE enzyme, and both IC_{50} and K_i values were calculated.

Molecular Docking

The interaction of compound **6e** with the AChE enzyme was investigated in molecular docking with *in silico* approaches. Molecular docking studies were applied to determine the amino acid residues in the active site of compound **6e** and the reference compound Tacrine and to calculate the binding parameters. Schrödinger 2021-2 software (Schrödinger Release 2021-2: Glide) was used in all docking studies to investigate the binding mode.

Molecular docking procedures specified in previous studies were applied (Anil, Aydin, Demir, & Turkmenoglu, 2022; Çöl, Bozbey, Türkmenoğlu, & Uysal, 2022a). The possible conformations of the studied compound were optimized using the "Ligand preparation wizard" program of Schrödinger 2021-2 (Schrödinger Release 2021-2: LigPrep). Possible tautomeric states of pH 7.0 ± 2.0 in the Epic ligand preparation portion were used to generate a net negative substitution change that varied in each case.

The AChE crystal structure was obtained from the protein database (https://www.rcsb.org/structure) and the crystal structure with PDB code number 1ACJ (Harel et al., 1993) was used. The crystal structure was prepared with the "Protein Preparation Wizard" interface of Schrödinger 2021-2 software (Schrödinger Release 2021-2: Protein Preparation Wizard; Epik). It was prepared by sequential processes such as deletion of water molecules, the addition of missing side chains and hydrogen atoms, protonation states, assignment of partial charges, optimization, and minimization using the OPLS-2005 force field.

Prime MM/GBSA (Schrödinger Release 2021-2: Prime)analysis was used to calculate ligand binding energies using the OPLS_2005 force field and the VSGB solvent model. MM/GBSA analysis was applied to determine the free binding energy of compound **6e** and the AChE crystal structure by molecular docking.

RESULTS AND DISCUSSION

Chemistry

In this study, five new AChE enzyme inhibitor compounds were synthesized (Figure 1) according to the general synthesis method outlined in Figure 2 and their anticholinesterase activities were examined. In the synthesis of the compounds, the 3(2*H*)-pyridazinone ring, which our study group worked on, was chosen as the main structure. In previous studies, hydrazone derivatives and sulfonyl hydrazide derivatives bearing pyridazinone ring were studied. In this study, these structures were modified and the triazole ring system was added to the general structure.

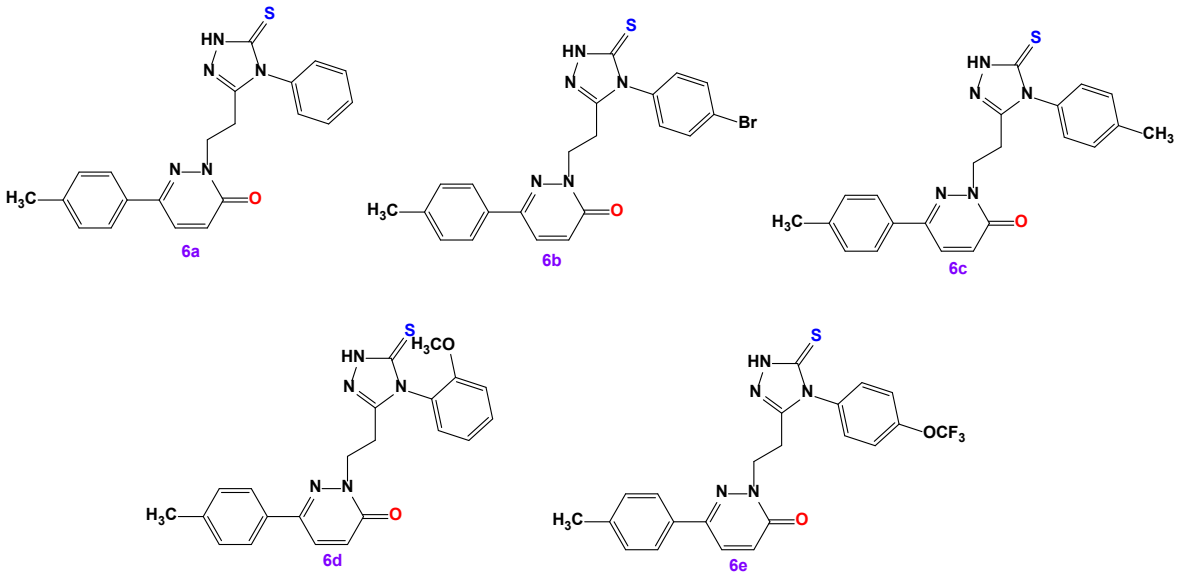


Figure 1. Synthesized compounds

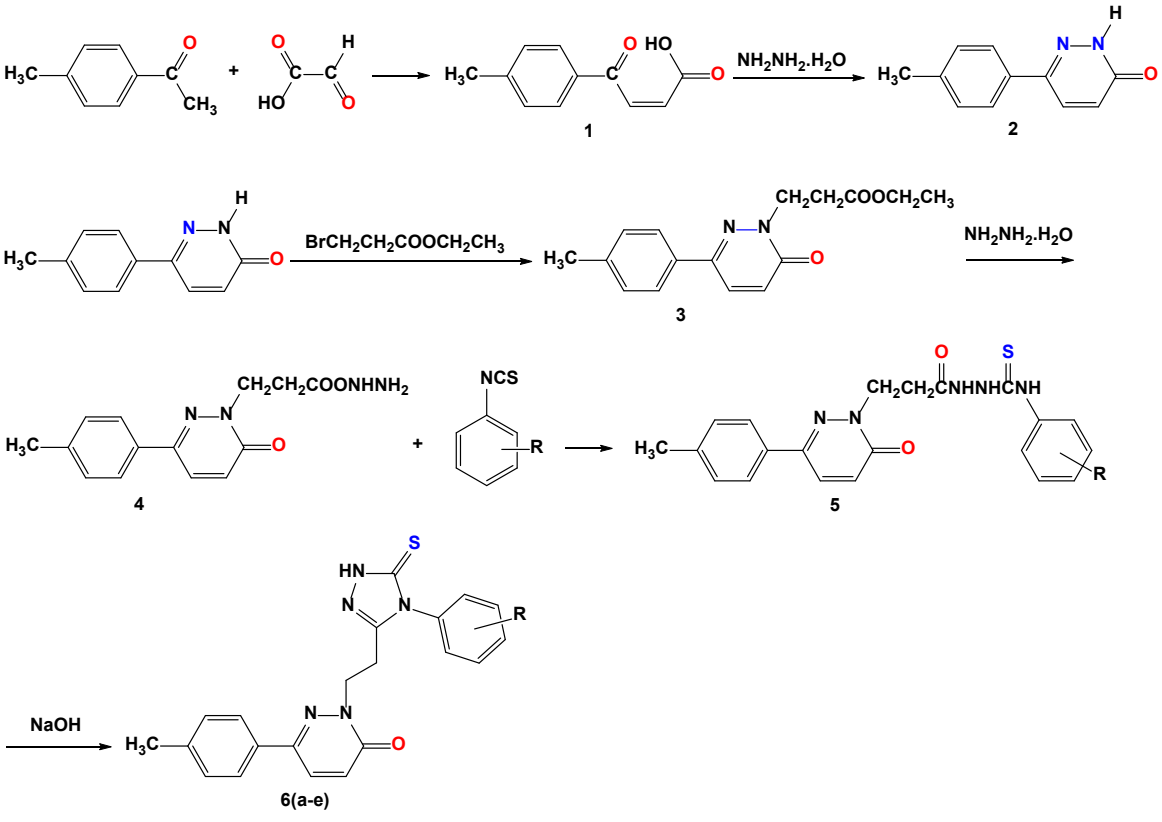


Figure 2. General synthesis method

The White-colored compounds **6**(**a**-**e**) were synthesized in yields ranging from 56-37% in general. The range of 13.67-11.72 ppm in the ^{1}H NMR spectrum showed triazole-N*H* peaks. Bridge of triazole and pyridazinone rings -CH_2CH_2- multiplet or triplet peaks were generally observed near 4.2-2.8 ppm in proton NMR (Figure 3). In the ^{13}C NMR spectrum, the pyridazinone ring carbonyl carbon supported structure accuracy in the range of 159.33-145.93 ppm. The specific thiocarbonyl group of the triazole ring was observed in the range of 168.49-160.82 ppm (Figure 4). In the FT-IR spectra, newly synthesized compounds **6**(**a**-**e**) exhibited characteristic ν(C=O) bands at 1654-1635 cm^{-1} for pyridazinone rings. The ν(N—H) stretching bands of the triazole rings were centered at 3220-3145 cm^{-1}. In addition, characteristic ν(C=S) bands were observed at 1164-1125 cm^{-1} (Figure 5).

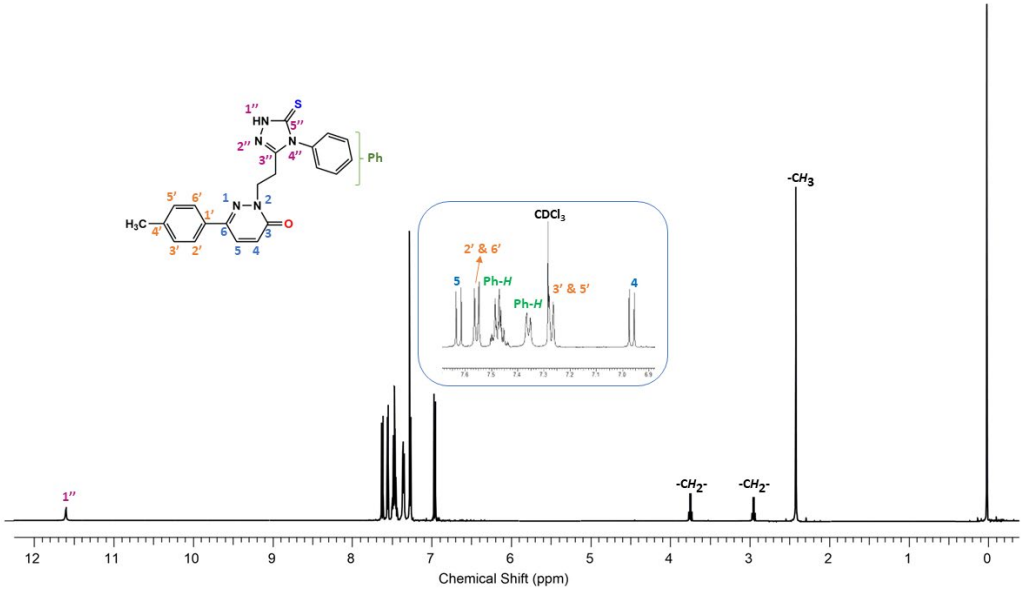


Figure 3. ^{1}H-NMR spectrum of compound **6a**

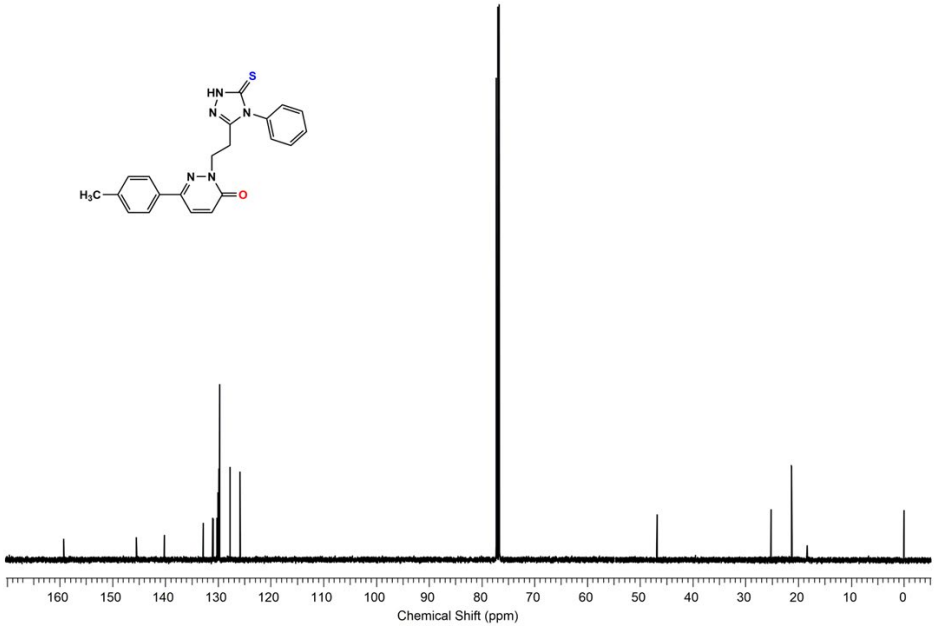


Figure 4. ^{13}C-NMR spectrum of compound **6a**

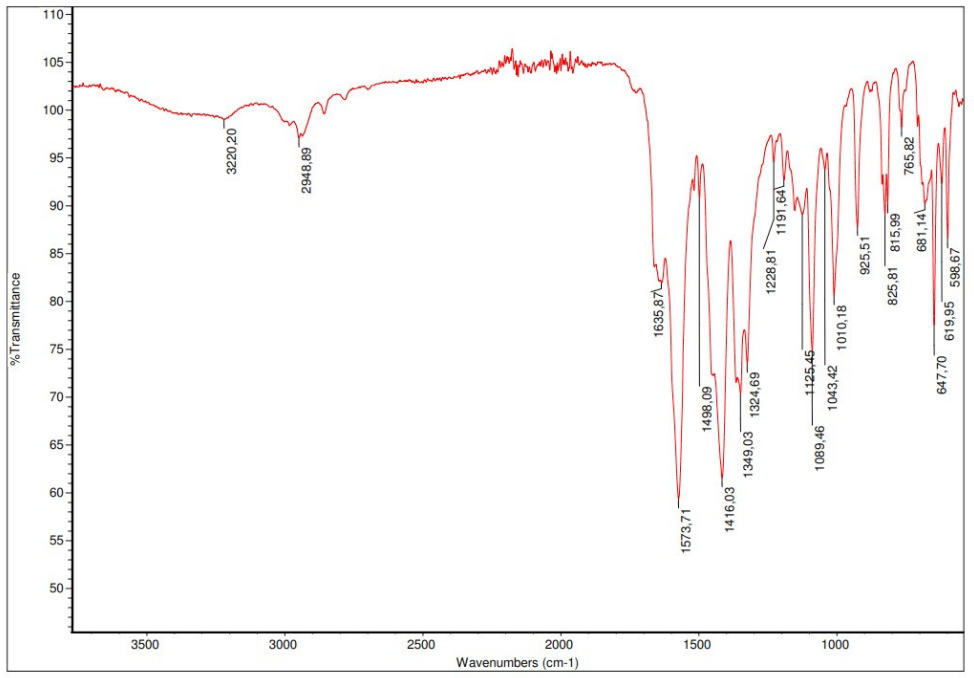


Figure 5. ATR-IR spectrum of compound **6a**

Biological evaluation and structure-activity relationship

IC_{50}, K_i, and inhibition types of five newly synthesized triazole-pyridazinone derivative compounds were determined. These values of the compounds are given in Table 1 and the IC_{50} graph and Lineweaver-Burk graph (B) of **6e** and Tacrine for AChE (Figure 6 and Figure 7). The IC_{50} values of the compounds were found as 0.310-0.592 μM and Ki values as 0.049 ± 0.014 - 0.484 ± 0.090 μM. The IC_{50} value of Tacrine, which we used as the reference compound, was determined as 0.519 μM and the Ki value as 0.226 ± 0.025 μM. When the contribution of the substituents to the structure was examined, the Ki value of the non-substituted compound **6a** was determined as 0.163 ± 0.017 μM. Compared to the non-substituted derivative (**6a**), 4-OCF_3 (**6e**) and 4-CH_3 (**6c**) groups in the structure increased the inhibitory effect, while the 4-Br (**6b**) and 2-OCH_3 (**6d**) groups decreased the inhibitory effect. The compound with the strongest inhibitory effect compared to Tacrine is compound **6e** with a Ki value of 0.049 ± 0.014 μM. These compounds were followed by **6c** and **6a** with Kı values of 0.098 ± 0.009, and 0.163 ± 0.017. The effect of the substituents on AChE activity was **6e** (4-trifluoromethoxy derivative) > **6c** (4-methyl derivative) > **6a** (non-substituted) > **6d** (2-methoxy derivative) > **6b** (4-bromo derivative). The inhibition type of compound **6a** was determined competitively as the reference compound Tacrine. In summary, especially the trifluoromethoxy substitute positively affected the activity.

Table 1. The IC_{50} values, K_i constants and inhibition types were determined for **6(a-e)** molecules having inhibitory effects on AChE.

Compound	AChE			
	IC_{50} (µM)	R^2	K_i (µM)	Inhibition Type
6a	0.474	0.9714	0.163 ± 0.017	Competitive
6b	0.551	0.9899	0.484 ± 0.090	Noncompetitive
6c	0.523	0.9713	0.098 ± 0.009	Uncompetitive
6d	0.592	0.9932	0.413 ± 0.093	Noncompetitive
6e	0.310	0.9747	0.049 ± 0.014	Uncompetitive
Tacrine	0.519	0.9257	0.226 ± 0.025	Competitive

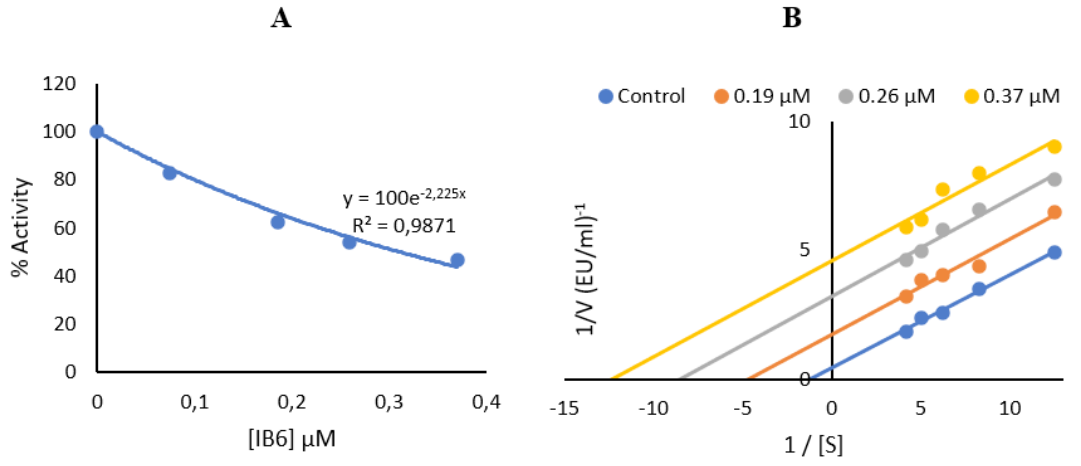


Figure 6. IC_{50} graph (A) and Lineweaver-Burk graph (B) of **6e** for AChE.

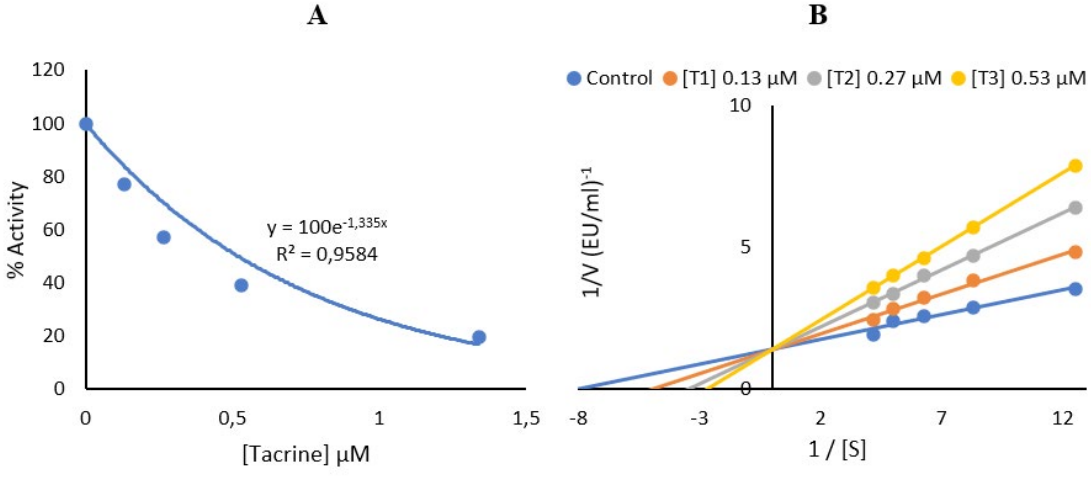


Figure 7. IC_{50} graph (A) and Lineweaver-Burk graph (B) of **Tacrine (TAC)** for AChE.

Molecular Docking

For the theoretical evaluation of the experimental activity of compound **6e** on AChE, binding interactions were determined by *in silico* approaches. Therefore, the crystal structure of the AChE enzyme (PDB ID: 1ACJ (Harel et al., 1993)) was used as the primary target for this study. The values of molecular docking results of **6e** and Tacrine compounds interacting with AChE, respectively, *in silico* approaches, were presented in Table 2.

Table 2. Binding parameter values as a result of *in silico* interaction of **6e** and Tacrine compounds with AChE crystal structure (PDB ID: 1ACJ (Harel et al., 1993)).

Parameters	6e	Tacrine
ΔG_{Bind} (kcal/mol)	-46.05	-32.14
Glide score (kcal/mol)	-8.850	-5.673
Docking score (kcal/mol)	-8.850	-5.673
Glide energy (kcal/mol)	-46.733	-32.657
Glide emodel (kcal/mol)	-44.843	-46.952

While designing compounds that can be new effective drug candidates, the results of the reference compounds used in the experimental activity are always taken into consideration. Therefore, molecular docking results of the compound synthesized with the reference compound with which the target interacts are important *in silico* approaches. Molecular docking results were none other than the binding parameter values shown in Table 2.

While the free binding energy of the binding parameters is -46.05 kcal/mol for compound **6e,** this value is -32.14 kcal/mol for Tacrine. When the glide score and docking score values are compared, it can be said, according to Table 1 that the docking score value of compound **6e** (-8.850 kcal/mol) is much better than the result of Tacrine (-5.673).

In addition, Glide energy and Glide emodel values, which are other important binding parameter values, were –46.733 kcal/mol and -44.843 kcal/mol for compound **6e**, respectively. These values were better than Tacrine.

The interactions with amino acid residues in the binding sites between the target and the ligand are as important as the binding parameters in the calculations for *in silico* approaches.

The 2D interaction diagram of **6e** and Tacrine compounds with the AChE crystal structure activated in molecular docking is presented in Figure 8. Figure 8(A) shows the amino acids in the active binding site in the 2D interaction diagram of **6e**, while Figure 8(B) shows the 2D interaction diagram of the PDB ID: 1ACJ (Harel et al., 1993) crystal structure interacting with the reference compound Tacrine.

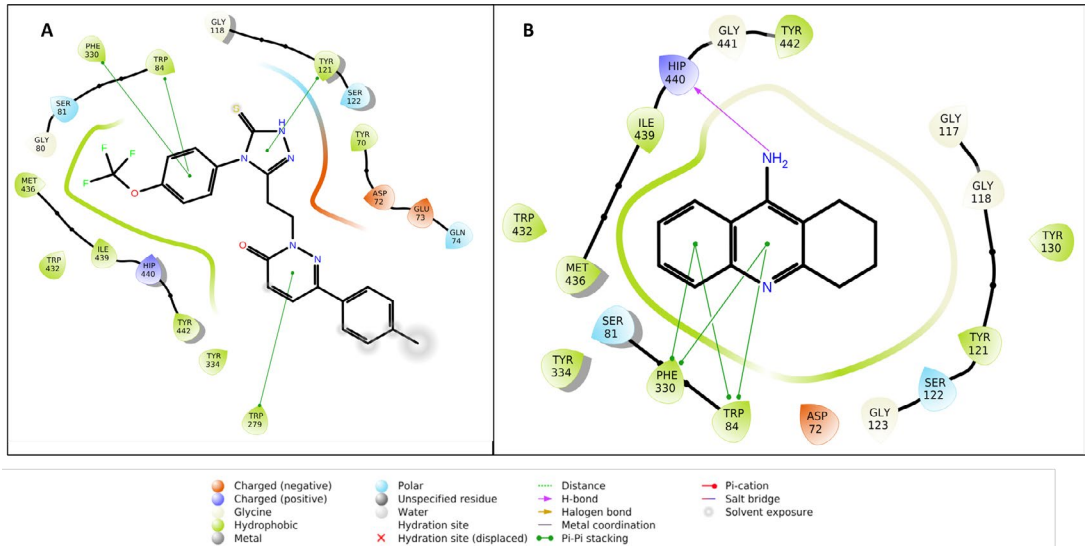


Figure 8. (A) 2D interaction diagram of **6e** compound with 1ACJ. (B) 2D interaction diagram of Tacrine with 1ACJ.

Figure 9 shows the 3D surface model structure of compound **6e** docked in the main groove of the 1ACJ crystal structure and the interaction of amino acid residues in its active binding site.

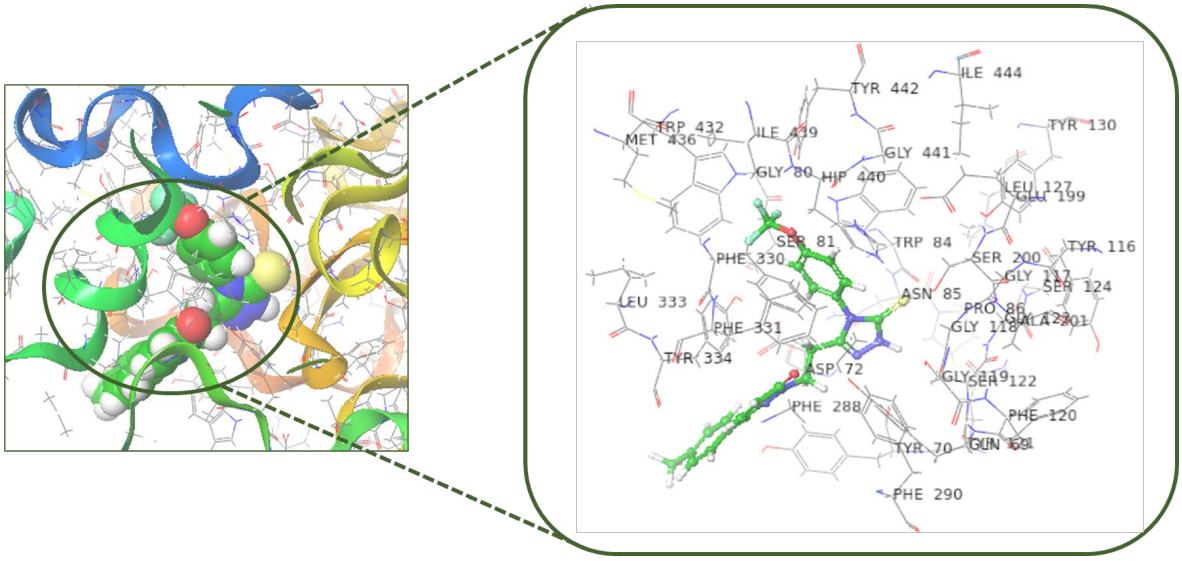


Figure 9. (A) Molecular docked structure of **6e** compound to 1ACJ crystal structure. (B) Amino acid residues at the binding site in the interaction of 1ACJ and **6e**.

In Figure 8(A), it was determined that compound **6e** interacts with the most important residues Trp 84, Phe 330 amino acid residues in this active site, in the binding site of AChE, and π- π interaction. In addition, the presence of π- π interaction of compound **6e** with Tyr 121 and Trp 279 is shown in Figure 8(A). Compound **6e** also appears to be well docked in the main cavity of the crystal structure. In Figure 8 (B), it is understood that the Tacrine compound makes **π-π** interaction with Trp84 and Phe 330, and hydrogen bond interaction with Hip 440. Molecular docking studies have been applied to understand the mechanism of action of **6e**, a compound that has the potential to act on AChE experimentally. For this reason, it can be said that the docking results of compound **6e** are better than Tacrine, the reference compound interacting with the target structure.

CONCLUSION

In summary, *in vitro* enzyme inhibitor activities were investigated by synthesizing five new compounds that we expect to have AChE enzyme inhibitor effects. The contribution of these groups to the activity was investigated by using non-substituted isothiocyanate, bromo, fluoro, methyl, methoxy and trifluoromethoxy substituted isothiocyanate derivatives in different positions in the synthesis of the derivatives. All synthesized derivatives **6(a-e)** were elucidated by spectroscopic analysis. Of the substituted pyridazinone derivatives, the p-trifluoromethoxy substituted derivative (**6e**) was found to be more potent against AChE inhibition. The molecular docking studies of the experimentally active compound **6e**, one of the compounds whose effects on the AChE enzyme were investigated, were investigated on the target crystal structure. It was noteworthy that Tacrine, the reference compound on the AChE enzyme, and compound 6e had similar binding sites and parameters. The results of the effect of compound 6e on the AChE enzyme, according to molecular docking with *in silico* approach, are promising.

ACKNOWLEDGEMENTS

The authors would like to thank Erzincan Binali Yıldırım University, Basic Sciences Application and Research Center (EBYU-EUTAM) for the Schrödinger Maestro 2021-2 program.

CONFLICT OF INTEREST

The authors declared no conflict of interest.

AUTHOR CONTRIBUTION STATEMENT

İ.B.M.; Conceptualization, Methodology, Resources, Writing – review & editing, Supervision, Visualization, G.T.Ö.; Conceptualization, Methodology, Resources, Writing – review & editing, Supervision, Visualization, B.T.; Methodology, Resources, Writing – review & editing, Visualization

Ş.G.; Resources, Writing – review & editing, Visualization, E.D.; Resources, Writing – review & editing, Visualization

REFERENCES

Anil, D. A., Aydin, B. O., Demir, Y., Turkmenoglu, B. (2022). Design, synthesis, biological evaluation and molecular docking studies of novel 1H-1, 2, 3-Triazole derivatives as potent inhibitors of carbonic anhydrase, acetylcholinesterase and aldose reductase. *Journal of Molecular Structure, 1257*, 132613.

Arora, K., Alfulaij, N., Higa, J. K., Panee, J., Nichols, R. A. (2013). Impact of sustained exposure to β-amyloid on calcium homeostasis and neuronal integrity in model nerve cell system expressing α4β2 nicotinic acetylcholine receptors. *J Biol Chem, 288*(16), 11175-11190. doi:10.1074/jbc.M113.453746

Birks, J. (2006). Cholinesterase inhibitors for Alzheimer‘s disease. *Cochrane Database Syst Rev, 2006*(1), Cd005593. doi:10.1002/14651858.Cd005593

Bozbey, İ., Özdemir, Z., Uslu, H., Özçelik, A. B., Şenol, F. S., Orhan İ, E., Uysal, M. (2020). A Series of New Hydrazone Derivatives: Synthesis, Molecular Docking and Anticholinesterase Activity Studies. *Mini Rev Med Chem, 20*(11), 1042-1060. doi:10.2174/1389557519666191010154444

Cummings, J., Lee, G., Zhong, K., Fonseca, J., Taghva, K. (2021). Alzheimer‘s disease drug development pipeline: 2021. *Alzheimers Dement (N Y), 7*(1), e12179. doi:10.1002/trc2.12179

Çöl, Ö. F., Bozbey, İ., Türkmenoğlu, B., Uysal, M. (2022b). 3(2H)-pyridazinone derivatives: Synthesis, in-silico studies, structure-activity relationship and in-vitro evaluation for acetylcholinesterase enzyme inhibition. *Journal of Molecular Structure, 1261*, 132970. doi:10.1016/j.molstruc.2022.132970

Daulatzai, M. A. (2016). Fundamental role of pan-inflammation and oxidative-nitrosative pathways in neuropathogenesis of Alzheimer‘s disease in focal cerebral ischemic rats. *American journal of neurodegenerative disease, 5*(2), 102-130.

Ellman, G. L., Courtney, K. D., Andres, V., Featherstone, R. M. (1961). A new and rapid colorimetric determination of acetylcholinesterase activity. *Biochemical Pharmacology, 7*(2), 88-95. doi:10.1016/0006-2952(61)90145-9

Fani Maleki, A., Cisbani, G., Plante, M.-M., Préfontaine, P., Laflamme, N., Gosselin, J., Rivest, S. (2020). Muramyl dipeptide-mediated immunomodulation on monocyte subsets exerts therapeutic effects in a mouse model of Alzheimer’s disease. *Journal of Neuroinflammation, 17*(1), 218. doi:10.1186/s12974-020-01893-3

Harel, M., Schalk, I., Ehretsabatier, L., Bouet, F., Goeldner, M., Hirth, C., ... Sussman, J. L. (1993). Quaternary Ligand-Binding to Aromatic Residues in the Active-Site Gorge of Acetylcholinesterase. *Proceedings of the National Academy of Sciences of the United States of America, 90*(19), 9031-9035. doi:10.1073/pnas.90.19.9031

Hassanien, A. Z. A. E.-B. (2003). Phthalazinone in Heterocyclic Synthesis: Synthesis of Some s-Triazole, s-Triazolothiadiazine, s-Triazolothiadiazine, and s-Triazolothiadiazole Derivatives as Pharmaceutical Interest. *Phosphorus, Sulfur, and Silicon and the Related Elements, 178*(9), 1987-1997. doi:10.1080/10426500390228666

Hosseini, S., Pourmousavi, S. A., Mahdavi, M., Taslimi, P. (2022). Synthesis, and in vitro biological evaluations of novel naphthoquinone conjugated to aryl triazole acetamide derivatives as potential anti-Alzheimer agents. *Journal of Molecular Structure, 1255*, 132229. doi:10.1016/j.molstruc.2021.132229

Huang, L.-K., Chao, S.-P., Hu, C.-J. (2020). Clinical trials of new drugs for Alzheimer disease. *Journal of biomedical science, 27*(1), 18. doi:10.1186/s12929-019-0609-7

Koronyo-Hamaoui, M., Sheyn, J., Hayden, E. Y., Li, S., Fuchs, D.-T., Regis, G. C., ... Rentsendorj, A. (2020). Peripherally derived angiotensin converting enzyme-enhanced macrophages alleviate Alzheimer-related disease. *Brain, 143*(1), 336-358. doi:10.1093/brain/awz364

Krasiński, A., Radić, Z., Manetsch, R., Raushel, J., Taylor, P., Sharpless, K. B., Kolb, H. C. (2005). In Situ Selection of Lead Compounds by Click Chemistry: Target-Guided Optimization of Acetylcholinesterase Inhibitors. *Journal of the American Chemical Society, 127*(18), 6686-6692. doi:10.1021/ja043031t

Kumar, K., Kumar, A., Keegan, R. M., & Deshmukh, R. (2018). Recent advances in the neurobiology and neuropharmacology of Alzheimer‘s disease. *Biomed Pharmacother, 98*, 297-307. doi:10.1016/j.biopha.2017.12.053

Mantu, D., Luca, M. C., Moldoveanu, C., Zbancioc, G., Mangalagiu, II. (2010). Synthesis and antituberculosis activity of some new pyridazine derivatives. Part II. *Eur J Med Chem, 45*(11), 5164-5168. doi:10.1016/j.ejmech.2010.08.029

Onkol, T., Doğruer, D. S., Uzun, L., Adak, S., Ozkan, S., Sahin, M. F. (2008). Synthesis and antimicrobial activity of new 1,2,4-triazole and 1,3,4-thiadiazole derivatives. *J Enzyme Inhib Med Chem, 23*(2), 277-284. doi:10.1080/14756360701408697

Özçelik, A. B., Özdemir, Z., Sari, S., Utku, S., Uysal, M. (2019). A new series of pyridazinone derivatives as cholinesterases inhibitors: Synthesis, in vitro activity and molecular modeling studies. *Pharmacological Reports, 71*(6), 1253-1263. doi:10.1016/j.pharep.2019.07.006

Saeedi, M., Maleki, A., Iraji, A., Hariri, R., Akbarzadeh, T., Edraki, N., ... Mirfazli, S. S. (2021). Synthesis and bio-evaluation of new multifunctional methylindolinone-1,2,3-triazole hybrids as anti-Alzheimer‘s agents. *Journal of Molecular Structure, 1229*, 129828. doi:https://doi.org/10.1016/j.molstruc.2020.129828

Saeedi, M., Safavi, M., Karimpour-Razkenari, E., Mahdavi, M., Edraki, N., Moghadam, F. H., ... Akbarzadeh, T. (2017). Synthesis of novel chromenones linked to 1,2,3-triazole ring system: Investigation of biological activities against Alzheimer‘s disease. *Bioorg Chem, 70*, 86-93. doi:10.1016/j.bioorg.2016.11.011

Schrödinger Release 2021-2: Glide, S., LLC, New York, NY, 2021.

Schrödinger Release 2021-2: LigPrep, S., LLC, New York, NY, 2021.

Schrödinger Release 2021-2: Prime, S., LLC, New York, NY, 2021.

Schrödinger Release 2021-2: Protein Preparation Wizard; Epik, S., LLC, New York, NY, 2021; Impact, Schrödinger, LLC, New York, NY; Prime, Schrödinger, LLC, New York, NY, 2021.

Shirinzadeh, H., Dilek, E., Alım, Z. (2022). Evaluation of Naphthalenylmethylen Hydrazine Derivatives as Potent Inhibitors on, Antiatherogenic Enzymes, Paraoxonase I and Acetylcholinesterase Activities. *ChemistrySelect, 7*(5), e202104489. doi:10.1002/slct.202104489

Srivastava, S., Ahmad, R., Khare, S. K. (2021). Alzheimer's disease and its treatment by different approaches: A review. *Eur J Med Chem, 216*, 113320. doi:10.1016/j.ejmech.2021.113320

Taudorf, L., Nørgaard, A., Waldemar, G., Laursen, T. M. (2021). Mortality in Dementia from 1996 to 2015: A National Registry-Based Cohort Study. *Journal of Alzheimer's disease : JAD, 79*(1), 289-300. doi:10.3233/JAD-200823

Xu, Q., Wang, Y., Xu, J., Sun, M., Tian, H., Zuo, D., ... Zhang, W. (2016). Synthesis and Bioevaluation of 3,6-Diaryl-[1,2,4]triazolo[4,3-b] Pyridazines as Antitubulin Agents. *ACS Medicinal Chemistry Letters, 7*(12), 1202-1206. doi:10.1021/acsmedchemlett.6b00252

Zhang, W., Jiao, B., Xiao, T., Liu, X., Liao, X., Xiao, X., ... Shen, L. (2020). Association of rare variants in neurodegenerative genes with familial Alzheimer's disease. *Annals of clinical and translational neurology, 7*(10), 1985-1995. doi:10.1002/acn3.51197